

Orbital Period and Outburst Luminosity of Transient Low Mass X-ray Binaries

Y. X. Wu^{1, 2}, W. Yu¹, T. P. Li^{2, 3, 4}, T.J. Maccarone⁵ and X. D. Li⁶

ABSTRACT

In this paper we investigate the relation between the maximal luminosity of X-ray outburst and the orbital period in transient low mass X-ray binaries (or soft X-ray transients) observed by the *Rossi X-ray Timing Explorer (RXTE)* in the past decade. We find that the maximal luminosity (3–200 keV) in Eddington unit generally increases with increasing orbital period, which does not show a luminosity saturation but in general agrees with theoretical prediction. The peak luminosities in ultra-compact binaries might be higher than those with orbital period of 2–4 h, but more data are needed to make the claim. We also find that there is no significant difference in the 3–200 keV outburst peak luminosity between neutron star systems and black hole systems with orbital periods above 4h; however, there might be significant difference at smaller orbital period where only neutron star systems are observed and radiatively inefficient accretion flow is expected to work at the low luminosities for black hole accreters.

Subject headings: accretion, accretion disks — binary: close — X-ray: binaries

1. Introduction

Low mass X-ray binaries (LMXB) contain primary stars which are either neutron stars (NSs) or black holes (BHs) and secondary stars typically less than $1 M_{\odot}$. The low mass companion stars are usually main sequence or subgiant stars, and also include white dwarfs or substellar mass

¹Shanghai Astronomical Observatory, 80 Nandan Road, Shanghai, 200030, China. E-mail: wenfei@shao.ac.cn

²Department of Engineering Physics & Center for Astrophysics, Tsinghua University, Beijing, China.

³Department of Physics & Center for Astrophysics, Tsinghua University, Beijing, China.

⁴Particle Astrophysics Lab., Institute of High Energy Physics, Chinese Academy of Sciences, Beijing, China.

⁵School of Physics and Astronomy, University of Southampton, Southampton, Hampshire SO17 1BJ, UK.

⁶Department of Astronomy, Nanjing University, Nanjing 210093, China.

objects. The secondary transfers matter to the NS or BH primary via Roche lobe overflow followed by disk accretion onto the primary. Soft X-ray transients (SXTs) are a subset of LMXBs which spend most of their time in quiescence, and occasionally exhibit outbursts during which their luminosities increase by several orders of magnitude (see reviews by Tanaka & Lewin 1995; van Paradijs & McClintock 1995; McClintock & Remillard 2006). During outbursts, SXTs go through a variety of “canonical” X-ray spectral states (see e.g. Tananbaum et al. 1972; van der Klis 1995; Fender et al. 2004a; McClintock & Remillard 2006; Done et al. 2007) based on their spectral and timing characteristics. The high/soft (HS) state corresponds to a relatively high luminosity, the X-ray spectrum dominated by a soft thermal component and $< \sim 5\%$ rms variability. The low/hard (LH) state, on the other hand, is characterized by a relatively low luminosity, the spectrum dominated by a hard non-thermal power-law component and $> \sim 20\%$ rms variability. There are also intermediate (IM) or very high (VH) states identified in the BH systems, of which the X-ray spectrum is composed of both a steep power-law component and a thermal component. SXTs usually enter the HS state from the LH state during the rising phase of an outburst and return to the LH state during the outburst decay. Past observations have also shown that a source can remain in the LH state throughout an outburst, which is usually of low luminosity (Brocksopp et al. 2006).

The most popular model for SXT outburst is the disk thermal instability (DTI) model (see the review of Lasota 2001, and references therein). In this model, for a certain range of surface density, the accretion disk can be either in a cool state where the gas is neutral or in a hot state where the gas is ionized. In the cool state the mass is accumulated in the disk until a surface density threshold is reached, above which only the hot state is possible. An outburst is then triggered, and the matter stored in the disk is accreted by the compact object. Although the model is generally adopted, diverse outburst properties are seen in the same source during different outbursts, suggesting that the SXT outbursts are complex.

If during an outburst the compact star accretes all of the material stored in the accretion disk, the total output energy of the outburst should be proportional to the mass in the accretion disk, assuming that the radiative efficiencies of accretion process among different outbursts remain the same. If the outburst profiles are comparable and the peak luminosity is scaled to the total output energy during outburst, we expect a correlation between the outburst peak luminosity and the disk mass among outbursts. Previous X-ray observations have shown that this is probably true. In the special black hole transient GX 339–4, an empirical linear relation between the peak flux of the LH state at the beginning of an outburst and the outburst waiting time since the previous outburst, and a correlation between the peak flux of the LH state during an outburst rise and the outburst peak flux were found (Yu et al. 2007; Wu et al. 2009). Actually the latter, namely the correlation between the luminosity of LH-to-HS state transition and the peak luminosity of the following HS state, has been confirmed for about 20 persistent and transient Galactic X-ray binaries in a luminosity range spanning by 2 orders of magnitude (Yu & Yan 2009). Combining the two correlations, we

expect a positive correlation between the outburst peak luminosity and the mass stored in the disk responsible for a certain outburst.

The maximal mass that can be stored in the disk before an outburst is limited by the size of the Roch-lobe in these LMXBs. The size of the Roch-lobe is reflected in the orbital period (P_{orb}). The binary separation is given by P_{orb} based on the Kepler’s law, and the Roche geometry is further determined by the binary separation and the mass ratio of the primary and the secondary (see Frank et al. 1992). In various models, the radial size of the accretion disk has a close relation with P_{orb} (see, e.g. Paczynski 1977; Whitehurst 1988; Lubow 1991; Frank et al. 1992), and in general a longer P_{orb} indicates a larger radius allowed for the disk. The properties of the secondary for a given P_{orb} are predicted by binary evolution theory. The mean density ρ of the secondary which fills its Roche lobe satisfies the approximate relation of $\rho \cong 110P_{\text{hr}}^{-2} \text{ g cm}^{-3}$, in which P_{hr} is P_{orb} in the unit of hours (Frank et al. 1992). The mechanisms driving the mass transfer in the binaries are different for different P_{orb} , which could be the expansion of the donor as it evolves away from the main sequence, or the loss of orbital angular momentum through gravitational radiation or magnetic braking (e.g., King 1988; King et al. 1996). The amount of mass in the accretion disk has been suspected to increase with increasing P_{orb} and primary mass (see, e.g. Meyer-Hofmeister & Meyer 2000; Portegies Zwart et al. 2004).

Theoretical calculation in Meyer-Hofmeister (2004) showed that the outburst peak luminosity varies with P_{orb} . Portegies Zwart et al. (2004) studied the BH transients in Garcia et al. (2003) and showed that the peak luminosity indeed varies with P_{orb} , but not exactly as the theories predicted. Similar study was also performed by Shahbaz et al. (1998) with the peak luminosity taken from Chen et al. (1997) (hereafter CSL97). It is worth noting that the theoretical relations between P_{orb} , the mass in the disk and the outburst peak luminosity can only hold in an average sense since SXT outburst varies from one to another, and the Eddington limit on the outburst peak luminosities in both the LH state and the HS state would cause a flat top of the outburst peak luminosity because of luminosity saturation, although this probably has not been seen (e.g., Yu & Yan 2009).

CSL97 presented a systematic study of the light curves of SXT outbursts before the *RXTE* era. Those transient outbursts were observed by *Ariel 5*, *EXOSAT*, *Ginga*, *CGRO* and so on from the 1960s to the middle 1990s. In the past decade, X-ray observations of transient sources have been greatly enriched. The missions such as *BeppoSAX*, *RXTE*, *INTEGRAL* and *Swift* have discovered dozens of new transients. Among them, *RXTE* has performed a lot of sensitive, pointed observations of transient outbursts in the past 15 years. A comprehensive study of these SXT outbursts observed with *RXTE* is very necessary. In this paper, we present our systematic study of the peak luminosity, the maximal HS state luminosity and the maximal LH state luminosity (in Eddington unit) in relation to P_{orb} for the transient sources listed in the LMXB catalogue by Liu et al. (2007) (hereafter LPH07).

2. Data Analysis and Results

2.1. Source Selection

Our source selection is based on the catalogue of LMXBs (LPH07). We first selected sources identified as transients with known orbital period P_{orb} . We obtained a list of 40 sources, 20 of which contain a BH or a BHC and the other 20 are thought to contain a NS. This led to the initial sample, in which 22 sources were listed in CSL97, including 17 confirmed SXTs and 5 possible SXTs. Among the 5 possible SXTs, 3A 1516-569, known as Cir X-1, probably consists of a subgiant companion star with a mass of 3–5 M_{\odot} or even higher (Johnston et al. 1999; Jonker et al. 2007a), and its periodic outbursts are often suggested to be the result of a highly eccentric orbit, rather than disk ionization instability. We excluded it from our source list. The other 4 sources, namely MXB 1659-298, 4U 1659-487 (GX 339-4), 1A 1744-361, and GS 1826-238, either have been taken as SXTs (e.g. Homan et al. 2005; Bhattacharyya et al. 2006) or have shown clear similarities to SXTs, so we included them. The remaining 18 sources in the list of 40 sources were not recorded in CSL97. GRO J1744-28 is excluded due to its characteristics of both a pulsar and a type II burster (e.g. Kouveliotou et al. 1996; Giles et al. 1996; Strickman et al. 1996; Cannizzo 1996). 4U 1755-33 and GRS 1747-312 are included in our sample because their transient natures are not distinct from SXTs. The other 15 sources, including 7 accretion-powered millisecond pulsars (APMSPs), were discovered after 1996 and are contained in our study. APMSP here refers to those showing persistent (the first six APMSPs) or predominant episodes (HETE J1900.1-2455) of pulsations during outbursts, rather than burst oscillations or the more recent intermittent pulsations seen in Aql X-1 and the NGC 6440 X-ray source (Casella et al. 2008; Altamirano et al. 2008). SWIFT J1756.9-2508 (Krimm et al. 2007) is the eighth APMSP but not taken into account due to its unknown distance. In total, our sample includes 38 sources (20 BH or BHC systems and 18 NS systems) with known P_{orb} (see Table 1). We have 3 more BHs and BHCs than the list in McClintock & Remillard (2006) (hereafter MR06).

In Table 1 we list the X-ray flux (the peak flux or the observed flux in the range between 2-10 keV, unless otherwise indicated), the mass, the distance and the orbital period taken from LPH07 for each of sources we selected.

2.2. Flux Measurements from the *RXTE* PCA and *HEXTE* Energy Spectra

As shown in the second column in Table 1, no outburst was seen in some of the sources in the past decade. On the other hand, two recently discovered sources CXOGC J174540.0-290031 and AX J1745.6-2901 lack *RXTE* pointed observations. This leaves a list of 25 sources whose outbursts have been observed with the *RXTE* pointed observations, among which 9 are BH systems and 16

are NS systems.

In order to estimate the outburst peak fluxes of these sources with *RXTE* pointed observations, for each source we first determined the date of the brightest outburst peak from all the PCA observations in 2–9 keV from daily averaged PCA light curves. This was checked with the *RXTE*/ASM light curve to guarantee that the date identification is correct. For those sources discovered before the *RXTE* era, the brightest outburst may be not the ones observed by the *RXTE*. One example is GS 1354-64, which showed a bright outburst entering the HS state in February, 1987 and a dim LH state outburst in November, 1997. We only determined the outburst peak flux with the *RXTE* observations. For some other sources, the corresponding *RXTE* observations may not cover the peak of the brightest outburst. For instance, the *RXTE* observations of IGR J00291+5934 and XTE J2123-058 only covered the outburst decays. In such cases, we took the first observation of each source to estimate the outburst peak flux. In some NS systems there were type I X-ray bursts. While the PCA daily averaged rates include photon counts from type-I X-ray bursts, the contribution from bursts is small. For the four sources in which bursts contributed to the peak rates – SAX J1808.4-3658, XTE J1814-338, GS 1826-238 and HETE J1900.1-2455 – we checked the light curves to make sure that we choose the observations consistent with the maximal persistent PCA count rates. We then entered the date corresponding to the observation of the outburst peak for each of the 25 sources in Table 2.

The hardness ratios between the HEXTE (15-250 keV) and PCA (2-9 keV) count rates were used to determine the spectral states as in previous works (e.g. Yu & Dolence 2007). The hardness ratios in the LH state (on the order of 0.1) are ten times those of the HS states (typically around 0.01). The VH state in BH systems has a hardness ratio between those of the LH state and the HS state, associated with a flux spike in the light curve. An outburst peak of BH transients could be any of the three states, and that of NSs could be either the LH state or the HS state. We identified the spectral state corresponding to each outburst peak (Table 2). In order to compare the peak fluxes of the same states in different sources, we also analyzed the observations corresponding to the maximal fluxes of different states if data permit. The maximal flux of the LH state during the rise or the decay of an outburst is marked as “r” or “d” in Table 2. Because the LH-to-HS state transition during an outburst rise occurs usually at a higher flux than the HS-to-LH state transition during the decay (known as “hysteresis”, e.g. Miyamoto et al. 1995; Nowak 1995; Homan et al. 2001; Smith et al. 2002; Maccarone & Coppi 2003), the HS-to-LH state transition flux was taken as the lower limit of the maximal flux of the LH state in case that the LH-to-HS state transition during the rise was not covered by the *RXTE* pointed observations. We also cross-checked with previous studies (e.g. Park et al. 2004 for 4U 1543-47; Sobczak et al. 2000 for XTE J1550-564; Miller et al. 2002 for XTE J1650-500; Brocksopp et al. 2006 and Shaposhnikov et al. 2007 for GRO J1655-40; Belloni et al. 2005 for GX 339-4; Yu & Dolence 2007 for Aql X-1) to make sure that our identifications of spectral states were correct.

Next we analyzed the spectra of the selected observations to derive the peak flux of the corresponding LH or HS state. The PCA/HEXTE spectra provided as the *RXTE* standard products were fitted with simple models. To ensure that the standard product provides the representative energy spectrum, we checked the data to make sure that the source flux is relative constant during the corresponding observation and consistent with flux peak. The PCA spectra in 3–25 keV and HEXTE spectra above 20 keV were analyzed jointly, by including a multiplicative factor to account for different calibrations of the two instruments. A systematic error of 1% was added to the PCA/HEXTE data. The model consisting of a multicolor blackbody (“diskbb” in Xspec) plus a power-law was applied to BH systems, and the model composed of a blackbody plus a power-law was used for NS systems. A gaussian line with the energy bounded between 5.9 and 6.9 keV was sometimes included additionally to describe an iron emission line component. In some cases the fits were significantly improved by including a Fe absorption edge or a smeared edge near 8 keV, or by replacing the power-law with a cutoff power-law. The former was usually found in bright sources and the latter in NS sources. Interstellar absorption was modeled using the Wisconsin cross section (“wabs” in Xspec). The hydrogen column density in the direction of a certain source was fixed at the value taken from the N_{H} tool provided by HEASARC website (<http://heasarc.gsfc.nasa.gov/cgi-bin/Tools/w3nh/w3nh.pl>) (Kalberla et al. 2005; Dickey & Lockman 1990). The best-fitting spectral parameters were listed in Table 2. The total unabsorbed X-ray flux between 3–200 keV for each observation was derived (see Table 3). Considering that the HEXTE spectrum in high energy band is dominated by the contribution of background and might essentially add noise in some cases, we also investigated if we cut off the HEXTE spectrum at the energy where the source counts fall to less than 20% of the background level (typically at 30–40 keV), what the flux with the best-fitting model extrapolated to 200 keV would be. We found the difference is less than 0.5%, so we analyzed the energy spectra in the 3–200 keV throughout to estimate the energy fluxes in the 3–200 keV range.

2.3. Luminosity Estimates

We calculated the X-ray luminosity in Eddington unit based on

$$\frac{L}{L_{\text{Edd}}} = \frac{F \times 4\pi D^2}{1.3 \times 10^{38} M}$$

in which F is the X-ray flux obtained in the spectral analysis, D is the source distance, M is the mass of the compact star in the unit of solar mass.

The uncertainties in the luminosity come from the uncertainties in the mass, the source distance and the source flux, among which the uncertainties in the mass and distance play a dominant role. BH mass values and their uncertainties were mostly taken from LPH07, but for

XTE J1118+480 and GRO J1655-40, we also used the mass range from MR06 in our study. The BH mass of XTE J1859+226 was taken from MR06. On the other hand, only the mass function are known for GS 1354-64 and 4U 1659-487. So we only had the lower limits on their BH masses. The source distances listed in LPH07 and MR06 are generally consistent. But for XTE J1859+226 the distances are different, and we used both in our study.

NS masses are not well measured in the transient LMXBs studied here. Common understanding is that NSs have a canonical mass of about $1.4 M_{\odot}$, but recent studies showed evidences for larger neutron star masses in a few systems – up to around $2 M_{\odot}$ (e.g., $1.86 \pm 0.6 M_{\odot}$ for Vela X-1, Barziv et al. 2001; $2.4 \pm 0.3 M_{\odot}$ for 4U 1700-37, Clark et al. 2002; $> 1.6 M_{\odot}$ for Aql X-1, Cornelisse et al. 2007). Theory allows for more than $2 M_{\odot}$ of maximal NS mass under some reasonable equations of state (e.g., see the review of Heiselberg & Pandharipande 2000, and references therein). We therefore assumed a NS mass range of 1.4 to $2.2 M_{\odot}$ for all the NS LMXBs except XTE J2123-058, which has a better mass estimate. The distances of NS systems were taken from LPH07.

We calculated source luminosities from the flux measurements. The outburst peak luminosity, the maximal HS state luminosity and the maximal LH state luminosity in Eddington unit as a function of P_{orb} are plotted in Figure 1–3, respectively. We mark each source as a number for a BH or a letter for a NS, which are shown in the first column of Table 3 as well. For most sources of which only a mass range or distance range is known, we plot the corresponding luminosity range as a solid line and the uncertainty range as a dotted line. The upper or lower limit on luminosity is shown as an arrow. The results are plotted as double arrows for GS 1354-64 (“2”) and 4U 1659-487 (“7”), because both their masses and distances are given as lower limits and therefore the luminosity estimates are not certain. For XTE J1807-294 (“j”), a distance of 8 kpc is assumed, hence it is marked with double arrows. The luminosities of the above three sources are only shown in the plot, but not used in our further analysis. It is worth noting that the luminosity of the HS-to-LH state transition during the decay of outburst was taken as the lower limit of the maximal LH state luminosity due to the hysteresis effect.

We made a comparison between the peak luminosities derived here and those in the classical work of CSL97. Table 8 in CSL97 listed the value of $\log(L_p/L_{\text{Edd}})$ for 24 transient sources, whose outbursts were detected between 1967 and 1996. Our results are more accurate in at least two aspects: 1) the energy band studied in CSL97 was 0.4–10 keV and the observed fluxes obtained by different X-ray instruments were converted to this energy range. While in our work the flux is measured through spectral modeling of the same instruments, with a broader energy coverage of 3–200 keV; 2) the uncertainties are estimated in our work, which are not present in CSL97. There are 6 sources covered by both samples. The maximal outburst peak luminosities of 4U 1543-47 and 4U 1608-52 in CSL97 are about twice as large as the corresponding values in our work. But in

logarithmic scale such differences would not significantly affect the overall relation. For the other four sources, the peak luminosities we measured are larger than or comparable to those in CSL97.

2.4. Outburst Peak Luminosity vs. Orbital Period

For the peak luminosity of each source, the corresponding luminosity range (hard boundary) and luminosity uncertainty range (soft boundary) are shown as a solid line and a dotted line in Figure 1, respectively. $L_{\text{peak}}/L_{\text{Edd}}$ on the whole is higher for a source with a larger P_{orb} , except the clear outlier XTE J1118+480 with P_{orb} of $\simeq 4.1$ h and L_{peak} of $\sim 0.001 L_{\text{Edd}}$. The highest $L_{\text{peak}}/L_{\text{Edd}}$ at the largest P_{orb} (GRS 1915+105, “9”) is close to the Eddington limit. In order to further investigate the statistical properties of these samples, we attempted to fit the relation on the logarithmic scale. The data with only upper or lower limits were excluded, the median value of the hard boundary was taken in the fitting, and the soft boundary was used to calculate the uncertainty. In the logarithmic axis the two-sided uncertainties would appear asymmetric and we used the larger one as the weight in the fitting.

First we fit with a straight line, which gives $\log L_{\text{peak}}/L_{\text{Edd}} = (-1.80 \pm 0.11) + (0.64 \pm 0.08) \log P_{\text{orb}}$ (see the upper left panel in Figure 4), with a reduced $\chi^2 = 28.1/18 = 1.56$. The significance of the F-test is 10^{-7} , rejecting the null hypothesis that the slope is zero for the overall sample. A positive correlation does exist for $L_{\text{peak}}/L_{\text{Edd}}$ and P_{orb} . We excluded the outlier XTE J1118+480 and fit again. The fit gives $\log L_{\text{peak}}/L_{\text{Edd}} = (-1.78 \pm 0.11) + (0.63 \pm 0.08) \log P_{\text{orb}}$, with a reduced $\chi^2 = 1.39$. The goodness of fit is improved but not significantly.

It appears that some sources in certain period regimes deviate from the linear relation. For example, not all the sources at small orbital periods show low luminosities. For the sources between 10 h and 100 h, the relation might be a “flat top” instead of a rise. Considering of these deviations, alternative models are also employed to fit the relation after excluding the outlier XTE J1118+480. The plot indicates that $L_{\text{peak}}/L_{\text{Edd}}$ may sharply increase at $P_{\text{orb}} \sim 5$ h. Therefore we tried the step function, i.e. a discontinuous fit with a smaller constant at short P_{orb} and a larger constant at long P_{orb} . The best-fitting result is (shown in the lower left panel in Figure 4)

$$\begin{cases} L_{\text{peak}}/L_{\text{Edd}} = 0.018 & \text{if } P_{\text{orb}} < 5 \text{ h} \\ L_{\text{peak}}/L_{\text{Edd}} = 0.145 & \text{if } P_{\text{orb}} \geq 5 \text{ h} \end{cases}$$

and the reduced $\chi^2 = 2.81$. The step function fit the data worse than the straight line. Allowing the reduced χ^2 increase by ~ 1 , we roughly estimated the uncertainties of the transition period as 5 ± 2 h. We modified the model as a linear model saturating at a constant at long P_{orb} . This model is used to describe the empirical relation of $\log L_{\text{peak}}/L_{\text{Edd}}$ and $\log P_{\text{orb}}$ for BH X-ray binaries in Portegies Zwart et al. (2004). The constant represents upper boundary for the transient luminosity.

Under this model fit, if the break period is not constrained, the best-fitting value of this parameter turns out to be very large, making it essentially a pure linear model. If we fixed the break period as 10 h as in Portegies Zwart et al. (2004), the best-fitting model can be expressed as (shown in the lower right panel in Figure 4)

$$\begin{cases} \log L_{\text{peak}}/L_{\text{Edd}} = 1.29 \log P_{\text{orb}} - 2.10 & \text{if } P_{\text{orb}} < 10 \text{ h} \\ \log L_{\text{peak}}/L_{\text{Edd}} = -0.81 & \text{if } P_{\text{orb}} \geq 10 \text{ h} \end{cases}$$

and the reduced $\chi^2 = 2.34$. We found that the linear model describes the relation best among the three models, in spite of the plausible deviations. Our fits do not support that there exists a break orbital period, or a saturated luminosity. The longest orbital period systems can be pushed up to Eddington luminosity or perhaps slightly above the Eddington luminosity, depending on the bolometric corrections.

We tried to investigate whether there is a systematic luminosity offset between BHs and NSs. We fixed the slope at 0.63, the best-fitting value for the overall data, and fit the data of BHs and NSs respectively. The results are shown in the upper right panel of Figure 4. The intercepts are -1.75 ± 0.11 for BHs and -1.79 ± 0.05 for NSs. They are consistent with being the same. We noticed that in the regime where P_{orb} is less than 4h, there are only NS sources, mostly APMSPs. We then fit the NS sources with P_{orb} larger than 4 h and got -1.75 ± 0.08 . Again, the intercepts of BHs and the NSs are consistent with the same. The absence of BH systems in the small P_{orb} regime may indicate that a BH system with a small P_{orb} tends to have outbursts with peak fluxes below the sensitivity of the X-ray monitoring missions in the past decade. This then implies that a systematic luminosity offset between the BHs and the NSs at low P_{orb} may exist, which is in the luminosity regime of below $\sim 0.01 L_{\text{Edd}}$.

We also studied the relation of the LH state peak luminosity $L_{\text{LH,max}}/L_{\text{Edd}}$ vs. the orbital period P_{orb} , and the HS state peak luminosity $L_{\text{HS,max}}/L_{\text{Edd}}$ vs. P_{orb} . We could not determine whether the peak luminosity of the LH state is positively correlated with P_{orb} , probably because we lack the coverage of *RXTE* pointed observations.

3. Discussion

3.1. Comparison with Theory

It is not surprising that $L_{\text{peak}}/L_{\text{Edd}}$ tends to be larger for systems with longer P_{orb} . van Paradijs (1996) studied disk instability in SXTs and concluded that an accreting NS or BH system tends to be transient if the average mass transfer rate is below a critical value which increases with P_{orb} . This implies that we tend to see transient sources with a larger P_{orb} at a higher average mass

accretion rate. For most of the sources in our sample, the number of outbursts detected in the past decade are about a few. Their recurrence times should not differ too much and are roughly on the same order of magnitude. The outburst peak luminosity is expected to correlate with the average mass accretion rate for the sources we studied. Therefore we are likely to see a positive correlation between $L_{\text{peak}}/L_{\text{Edd}}$ and P_{orb} if the Eddington limit is not reached.

The trend is also expected from the theoretical calculation of King & Ritter (1998). They showed that the light curves of SXTs can be explained by disk instability if taking into account of irradiation by the central X-ray source during the outburst. If the luminosity is high, irradiation will be strong enough to ionize the entire disk and the X-ray light curve would be roughly an exponential decay. If the X-ray flux is too weak to ionize the whole disk, the outburst light curve should be roughly a linear decay. Based on (31) and (32) in King & Ritter (1998), the peak luminosities for an outburst with an exponential decay and linear decay can be calculated as

$$\begin{cases} L_{\text{p,exp}} = 2.7 \times 10^{38} R_{11}^{7/4} \text{ erg s}^{-1} \\ L_{\text{p,lin}} = 2.3 \times 10^{36} R_{11}^2 \text{ erg s}^{-1} \end{cases}$$

respectively. Here R_{11} is the maximal ionized disk radius in units of 10^{11} cm, which is roughly the maximum of the outer disk radius, usually taken as the tidal radius of the disk and estimated as 80% of the primary's Roche lobe radius. According to Eggleton (1983), the primary's Roche lobe radius can be calculated by the approximate analytic formula

$$R_1 = \frac{0.49aq^{-2/3}}{0.6q^{-2/3} + \ln(1 + q^{-1/3})},$$

in which q is the mass ratio between the secondary and the primary m_2/m_1 , and a is the binary separation which can be conveniently expressed in the form

$$a = 3.5 \times 10^{10} m_1^{1/3} (1 + q)^{1/3} P_{\text{orb}}^{2/3} \text{ cm}.$$

Assuming $q \sim 0.1$ and combining the above equations, we get

$$\begin{cases} L_{\text{p,exp}} = 1.18 \times 10^{37} m_1^{7/12} P_{\text{orb}}^{7/6} \text{ erg s}^{-1} \\ L_{\text{p,lin}} = 6.42 \times 10^{34} m_1^{2/3} P_{\text{orb}}^{4/3} \text{ erg s}^{-1}, \end{cases}$$

where m_1 is the primary mass in units of solar mass, and P_{orb} is the orbital period in units of hour. We plot the theoretical results as solid lines in Figure 5 together with the peak luminosities we measured. No source is observed beyond the maximal peak luminosity. At short P_{orb} , L_{peak} tends to be close to the theoretical peak luminosity corresponding to an outburst with an exponential decay, indicating that the disks in these systems are likely entirely irradiated. Systems with longer P_{orb} have L_{peak} close to the theoretical peak luminosity for a linear decay, probably because the disk in these systems are large and only the inner parts of the disks are irradiated. This is consistent with the prediction of King & Ritter (1998).

3.2. XTE J1118+480

Orbital period and peak luminosity in Eddington unit generally follow a positive correlation, whereas XTE J1118+480 is an outlier. Its 3–200 keV peak luminosity is only about $10^{-3}L_{\text{Edd}}$, one order of magnitude lower than the other sources with similar P_{orb} . The source is the BH SXT known with the shortest P_{orb} and almost the shortest distance, which remained in the LH state throughout the outburst we observed. During the outburst, it showed strong non-thermal radiation in the radio to optical band and a very low X-ray to optical flux ratio (e.g. Garcia et al. 2000). Another even fainter outburst was observed in January, 2005 (Remillard et al. 2005), which proves that such faint outburst is not occasional but typical for XTE J1118+480. Several physical interpretations have been proposed for this source, involving the radiative inefficient accretion flow (Esin et al. 2001), jet synchrotron radiation in the LH state (Markoff et al. 2001) and jet-disk coupling (Malzac et al. 2004). A popular idea is that the bolometric correction to its luminosity would be much larger than those for other sources which stayed in the LH state throughout an outburst. However, $L_{\text{peak}}/L_{\text{Edd}}$ of XTE J1118+480 is rather low even compared with the brightest LH state luminosities of other sources (Figure 3), which suggests alternative interpretations. One possibility is that the radiative efficiency for systems far from the critical luminosity of state transitions is lower than that for the brightest LH state systems — the advection dominated accretion flow model, for example, gives $L_X \propto \dot{m}^2$ (e.g. Esin et al. 1997). If this model applies to XTE J1118+480, then the radiative efficiency of this system might be a factor of ~ 5 smaller than the other black hole systems, putting its mass accretion rate much closer to the other systems than its luminosity.

3.3. Ultra-Compact Binary with Higher Luminosity?

In Figure 1 the complex phenomena below 4 h can be noticed: the peak luminosities for sources with orbital period between 2–4 h —namely IGR J00291+5934 (“a”), EXO 0748-676 (“b”), XTE J1710-281 (“f”) and XTE J1814-338 (“l”)—drop suddenly; while among the three sources with $P_{\text{orb}} < 1$ h, XTE J1751-305 (“i”) has a lower limit of $L_{\text{peak}}/L_{\text{Edd}}$ which is one order of magnitude larger than those between 2–4 h, and the other two might have higher $L_{\text{peak}}/L_{\text{Edd}}$ but accurate distance measurements are not available. It is an interesting question whether the ultra-compact X-ray binary with orbital period smaller than 1 h can reach higher peak luminosity than the source in the period range of 2–4 hours.

Only according to this work, the evidences are not conclusive due to the below considerations. In the first place the number of sources is not enough in statistics, and their masses and distances are quite uncertain. For example the distance of XTE J0929-314 (“c”), indicated as 10 ± 5 kpc in LPH07, seems to lack of solid observational basis. Secondly for very close binaries the donor

stars are likely to be hydrogen depleted, so that their Eddington luminosities are different from those in wider systems—in which accreting matter is hydrogen—by a factor of a few. As a result $L_{\text{peak}}/L_{\text{Edd}}$ plotted here are not the actual values for the ultra-compact binaries. Thirdly we notice that all the three ultra-compact binaries with orbital period lower than 1 h are APMSPs. There may be a selection effect at short orbital period regime since the short period were determined from X-ray pulse arrival times (e.g. Markwardt et al. 2002). At the same time these X-ray pulsars are very likely with non-isotropic emission from the polar region in addition to disk emission, and their apparent luminosities to the observer have a systematic increment. Lastly the low outburst peak luminosities observed in sources with orbital periods of several hours might be accidental. For example, IGR J00291+5934 (“a”) has a radio counterpart (Fender et al. 2004b) that indicates an outflow, which is likely radiatively inefficient. In addition, it might be at a larger distance than we thought (7–10 kpc, see Burderi et al. 2006). Both factors would cause the low luminosity – the former by reducing the intrinsic luminosity and the latter by underestimating the conversion factor from flux to luminosity. Another example is EXO 0748-676 (“b”). It has been observed with X-ray dips (Parmar et al. 1986); strong inclination effects may cause a lower luminosity as well. All the above factors would cause the ultra-compact binaries appear brighter than we expected from the empirical linear relation. Just based on our work it might be premature to claim that $L_{\text{peak}}/L_{\text{Edd}}$ in ultra compact binary system is essentially higher than that in the system not so compact. However it is a problem worthy of further investigation, because additional accretion stream component or slightly different accretion geometry might exist in ultra-compact X-ray binaries (e.g. Zhang et al. 2006).

3.4. BH and NS systems

An interesting investigation is a comparison of BH and NS systems. Menou et al. (1999) and Garcia et al. (2001) studied the quiescent luminosities of NS and BH SXTs as a function of P_{orb} , and found systematically higher quiescent luminosities for NS SXTs. This is consistent with the idea that the former has a hard surface and the later has an event horizon instead. However, further studies show that at least some of the NS SXTs can be as faint as BH SXTs in quiescence (e.g. Jonker et al. 2007b). In our study, we found no significant difference in the outburst peak luminosities between BHs and NSs systems at similar P_{orb} . This indicates that the radiative efficiencies of the accretion flows around NSs and BHs during the outburst peaks are comparable, probably except for the case of XTE J1118+480 discussed above.

It is worth noting that all the BH transients we studied have an orbital period larger than ~ 4 h. Significant difference in the radiation efficiencies between BH systems and NS systems at low luminosities and at small orbital periods can not be ruled out. BH transient systems with

$P_{\text{orb}} \lesssim 4\text{h}$ should have very faint outbursts. Because for short P_{orb} SXTs, they should have low mass transfer rate in order to remain as transients (van Paradijs 1996), about $1\% \dot{M}_{\text{Edd}}$ or below for BHs towards small P_{orb} ($\lesssim 4\text{h}$). At such a low mass accretion rate, the accretion flow would be radiatively inefficient and the observed luminosity is far less than $1\% L_{\text{Edd}}$. Therefore the BH systems are expected dimmer than the NS systems at short P_{orb} . XTE J1118+480, which is the faintest ($\sim 0.1\% L_{\text{Edd}}$, much smaller than other BHs) as well as the shortest-period BH in our sample, shows some evidence of radiatively inefficient accretion. This implies that few BH systems with an orbital period below 4h are observed may be the result of radiatively inefficient flow at low mass accretion rate in BH systems.

3.5. The Accretion Disk Mass

Evidence for the connection between the mass in the accretion disk when an outburst occurs and the peak luminosity of an outburst can be inferred from the observations of black hole transient GX 339-4 (Yu et al. 2007; Wu et al. 2009). For the same compact star mass and companion mass in a LMXB, P_{orb} indicates the size of the Roche lobe. The mass stored in the accretion disk during quiescence is then limited by the size of the Roche lobe. We show that there is an overall positive correlation between $L_{\text{peak}}/L_{\text{Edd}}$ and P_{orb} in transient LMXBs. This supports the idea that there is a correlation between the outburst peak luminosity and the initial mass in the accretion disk (Yu, van der Klis & Fender 2004; Yu et al. 2007; Yu & Yan 2009). A positive correlation between $L_{\text{peak}}/L_{\text{Edd}}$ and P_{orb} therefore strengthens that the mass in the accretion disk affects the outburst properties. Indeed, theoretical studies of SXT outbursts have shown that a positive correlation between $L_{\text{peak}}/L_{\text{Edd}}$ and P_{orb} exist for certain model parameters (Meyer-Hofmeister 2004). Taking into account that there is a correlation between the LH-to-HS transition luminosity, the rate-of-change of luminosity, and outburst peak luminosity in X-ray binaries (Yu & Yan 2009), the mass in the accretion disk seems the most important parameter that sets up the accretion processes during outbursts.

As shown above, the relation between the allowed maximal outer disk radius $R_{\text{max,disk}}$ and P_{orb} can be approximated as $R_{\text{max,disk}} \sim P_{\text{orb}}^{2/3}$. The best-fitting linear model in the logarithmic axis gives $L_{\text{peak}}/L_{\text{Edd}} \sim P_{\text{orb}}^{0.64}$. Combining them we obtained $L_{\text{peak}}/L_{\text{Edd}} \sim R_{\text{max,disk}}$, which indicate a nearly linear relation between the Eddington-scaled maximal peak luminosity and the allowed maximal outer disk radius. This is an interesting result and might provide constraints for some certain theoretical models and physical parameters. If total energy fluence of outburst is measured and total mass accreted to the compact star is estimated, the threshold of disk surface density for triggering outburst can be constrained.

4. Summary

We studied the relation between the outburst peak luminosity and the orbital period in transient LMXBs. We analyzed the PCA/HEXTE spectra of 25 LMXBs whose outburst peaks had been covered by *RXTE* pointed observations, and measured the peak flux of the brightest outburst of each source in the energy range between 3–200 keV. We then estimated the luminosities in Eddington unit as well as their uncertainties. The maximal luminosity of the LH and HS state were also studied as well.

We found that $L_{\text{peak}}/L_{\text{Edd}}$ on the whole is higher for sources with larger P_{orb} , showing no sign of luminosity saturation expected when approaching the Eddington limit towards larger P_{orb} . We fitted the relation in the logarithmic scale with three models: a straight line model, a step function model and a straight line connected with a constant model. The linear relation can well describe the data.

We find the theoretic work by King & Ritter (1998) is quantitatively consistent with the relation of peak luminosity and orbital period we obtained. The contrast at short orbital period regime might indicate that the ultra-compact binaries have unexpected higher luminosities which, however, is not conclusive only based on our study due to a number of observational uncertainties. We have also compared $L_{\text{peak}}/L_{\text{Edd}}$ of NS and BH SXTs, and found that generally there is no significant difference between them. Therefore radiative efficiencies of the accretion flows are comparable for NS and BH with similar P_{orb} during outburst peaks. Since we have not seen BH systems with P_{orb} less than 4h, it is possible that BH transients with short P_{orb} have lower outburst peak luminosities than the NS systems, because the accretion flow might be radiative inefficient at low mass accretion rate.

We would like to thank the *RXTE* Guest Observer Facilities at NASA Goddard Space Flight Center (GSFC) for providing the *RXTE* standard products and the ASM monitoring results. WY would like to thank Jean Swank and Craig Markwardt of GSFC for useful discussions and kind assistance. YW would like to thank Roberto Soria, Piergiorgio Casella, Tomaso Belloni, Shuang Nan Zhang and Hua Feng. This work was supported in part by the National Natural Science Foundation of China (including 10773023, 10833002), the One Hundred Talents project of the Chinese Academy of Sciences, the Shanghai Pujiang Program (08PJ14111), the National Basic Research Program of China (2009CB824800), and the starting funds of the Shanghai Astronomical Observatory. The study has made use of data obtained through the High Energy Astrophysics Science Archive Research Center Online Service, provided by the NASA/Goddard Space Flight Center.

REFERENCES

- Altamirano, D., Casella, P., Patruno, A., Wijnands, R., & van der Klis, M. 2008, *ApJ*, 674, L45
- Barziv, O., Kaper, L., Van Kerkwijk, M. H., Telting, J. H., & Van Paradijs, J. 2001, *A&A*, 377, 925
- Belloni, T., Homan, J., Casella, P., van der Klis, M., Nespoli, E., Lewin, W. H. G., Miller, J. M., & Méndez, M. 2005, *A&A*, 440, 207
- Bhattacharyya, S., Strohmayer, T. E., Markwardt, C. B., & Swank, J. H. 2006, *ApJ*, 639, L31
- Brocksopp, C., et al. 2006, *MNRAS*, 365, 1203
- Burderi, L., et al. 2006, *Chinese Journal of Astronomy and Astrophysics Supplement*, 6, 192
- Campana, S., Ravasio, M., Israel, G. L., Mangano, V., & Belloni, T. 2003, *ApJ*, 594, L39
- Cannizzo, J. K. 1996, *ApJ*, 466, L31
- Casares, J., Zurita, C., Shahbaz, T., Charles, P. A., & Fender, R. P. 2004, *ApJ*, 613, L133
- Casella, P., Altamirano, D., Patruno, A., Wijnands, R., & van der Klis, M. 2008, *ApJ*, 674, L41
- Chen, W., Shrader, C. R., & Livio, M. (CSL97) 1997, *ApJ*, 491, 312
- Clark, J. S., Goodwin, S. P., Crowther, P. A., Kaper, L., Fairbairn, M., Langer, N., & Brocksopp, C. 2002, *A&A*, 392, 909
- Cornelisse, R., Casares, J., Steeghs, D., Barnes, A. D., Charles, P. A., Hynes, R. I., & O'Brien, K. 2007, *MNRAS*, 375, 1463
- Dickey, J. M., & Lockman, F. J. 1990, *ARA&A*, 28, 215
- Done, C., Gierliński, M., & Kubota, A. 2007, *A&A Rev.*, 15, 1
- Eggleton, P. P. 1983, *ApJ*, 268, 368
- Esin, A. A., McClintock, J. E., Drake, J. J., Garcia, M. R., Haswell, C. A., Hynes, R. I., & Munro, M. P. 2001, *ApJ*, 555, 483
- Esin, A. A., McClintock, J. E., & Narayan, R. 1997, *ApJ*, 489, 865
- Falanga, M., et al. 2005, *A&A*, 436, 647
- Fender, R. P., Belloni, T. M., & Gallo, E. 2004a, *MNRAS*, 355, 1105

- Fender, R., De Bruyn, G., Pooley, G., & Stappers, B. 2004b, *The Astronomer's Telegram*, 361, 1
- Frank, J., King, A., & Raine, D. 1992, *Accretion Power in Astrophysics* (Cambridge: Cambridge Univ. Press)
- Garcia, M., Brown, W., Pahre, M., McClintock, J., Callanan, P., & Garnavich, P. 2000, *IAU Circ.*, 7392, 2
- Garcia, M. R., McClintock, J. E., Narayan, R., Callanan, P., Barret, D., & Murray, S. S. 2001, *ApJ*, 553, L47
- Garcia, M. R., Miller, J. M., McClintock, J. E., King, A. R., & Orosz, J. 2003, *ApJ*, 591, 388
- Giles, A. B., Swank, J. H., Jahoda, K., Zhang, W., Strohmayer, T., Stark, M. J., & Morgan, E. H. 1996, *ApJ*, 469, L25
- Heiselberg, H., & Pandharipande, V. 2000, *Annual Review of Nuclear and Particle Science*, 50, 481
- Homan, J., Buxton, M., Markoff, S., Bailyn, C. D., Nespoli, E., & Belloni, T. 2005, *ApJ*, 624, 295
- Homan, J., Wijnands, R., van der Klis, M., Belloni, T., van Paradijs, J., Klein-Wolt, M., Fender, R., & Méndez, M. 2001, *ApJS*, 132, 377
- Johnston, H. M., Fender, R., & Wu, K. 1999, *MNRAS*, 308, 415
- Jonker, P. G., Nelemans, G., & Bassa, C. G. 2007a, *MNRAS*, 374, 999
- Jonker, P. G., Steeghs, D., Chakrabarty, D., & Juett, A. M. 2007b, *ApJ*, 665, L147
- Kalberla, P. M. W., Burton, W. B., Hartmann, D., Arnal, E. M., Bajaja, E., Morras, R., & Pöppel, W. G. L. 2005, *A&A*, 440, 775
- King, A. R. 1988, *QJRAS*, 29, 1
- King, A. R., Kolb, U., & Burderi, L. 1996, *ApJ*, 464, L127
- King, A. R., & Ritter, H. 1998, *MNRAS*, 293, L42
- Kouveliotou, C., van Paradijs, J., Fishman, G. J., Briggs, M. S., Kommers, J., Harmon, B. A., Meegan, C. A., & Lewin, W. H. G. 1996, *Nature*, 379, 799
- Krimm, H. A., et al. 2007, *ApJ*, 668, L147
- Lasota, J.-P. 2001, *New Astronomy Review*, 45, 449

- Liu, Q. Z., van Paradijs, J., & van den Heuvel, E. P. J. 2007, *A&A*, 469, 807 (LPH07)
- Lubow, S. H. 1991, *ApJ*, 381, 268
- Maccarone, T. J., & Coppi, P. S. 2003, *MNRAS*, 338, 189
- Malzac, J., Merloni, A., & Fabian, A. C. 2004, *MNRAS*, 351, 253
- Markoff, S., Falcke, H., & Fender, R. 2001, *A&A*, 372, L25
- Markwardt, C. B., Swank, J. H., Strohmayer, T. E., in 't Zand, J. J. M., & Marshall, F. E. 2002, *ApJ*, 575, L21
- Masetti, N., Bianchini, A., Bonibaker, J., della Valle, M., & Vio, R. 1996, *A&A*, 314, 123
- McClintock, J. E., & Remillard, R. A. 2006, *Compact stellar X-ray sources*, 157 (MR06)
- Menou, K., Esin, A. A., Narayan, R., Garcia, M. R., Lasota, J.-P., & McClintock, J. E. 1999, *ApJ*, 520, 276
- Meyer-Hofmeister, E., & Meyer, F. 2000, *A&A*, 355, 1073
- Meyer-Hofmeister, E. 2004, *A&A*, 423, 321
- Miller, J. M., et al. 2002, *ApJ*, 570, L69
- Miyamoto, S., Kitamoto, S., Hayashida, K., Egoshi, W. 1995, *ApJ*, 442, L13
- Muno, M. P., Pfahl, E., Baganoff, F. K., Brandt, W. N., Ghez, A., Lu, J., & Morris, M. R. 2005, *ApJ*, 622, L113
- Nowak, M. A. 1995, *PASP*, 107, 1207
- Orosz, J. A., McClintock, J. E., Remillard, R. A., & Corbel, S. 2004, *ApJ*, 616, 376
- Paczynski, B. 1977, *ApJ*, 216, 822
- Park, S. Q., et al. 2004, *ApJ*, 610, 378
- Parmar, A. N., White, N. E., Giommi, P., & Gottwald, M. 1986, *ApJ*, 308, 199
- Portegies Zwart, S. F., Dewi, J., & Maccarone, T. 2004, *MNRAS*, 355, 413
- Remillard, R., Garcia, M., Torres, M. A. P., & Steeghs, D. 2005, *The Astronomer's Telegram*, 384,

- Shahbaz, T., Charles, P. A., & King, A. R. 1998, MNRAS, 301, 382
- Shahbaz, T., Naylor, T., & Charles, P. A. 1997, MNRAS, 285, 607
- Shaposhnikov, N., Swank, J., Shrader, C. R., Rupen, M., Beckmann, V., Markwardt, C. B., & Smith, D. A. 2007, ApJ, 655, 434
- Smith, D. M., Heindl, W. A., Swank, J. 2002, ApJ, 569, 362
- Sobczak, G. J., McClintock, J. E., Remillard, R. A., Cui, W., Levine, A. M., Morgan, E. H., Orosz, J. A., & Bailyn, C. D. 2000, ApJ, 544, 993
- Strickman, M. S., et al. 1996, ApJ, 464, L131
- Tanaka, Y., & Lewin, W. H. G. 1995, X-ray binaries, p. 126 - 174, 126
- Tananbaum, H., Gursky, H., Kellogg, E., Giacconi, R., & Jones, C. 1972, ApJ, 177, L5
- van der Klis, M. 1995, X-ray binaries, p. 252 - 307, 252
- van Paradijs, J. 1996, ApJ, 464, L139
- van Paradijs, J., & McClintock, J. E. 1995, X-ray binaries, p. 58 - 125, 58
- Whitehurst, R. 1988, MNRAS, 232, 35
- Wu, Y. X., Yu, W., Yan, Z., Sun, L., Li, T. P., submitted to A&A
- Yu, W., & Dolence, J. 2007, ApJ, 667, 1043
- Yu, W., Lamb, F. K., Fender, R., & van der Klis, M. 2007, ApJ, 663, 1309
- Yu, W., van der Klis, M. & Fender, R., 2004, ApJ, 611, L121
- Yu, W., & Yan, Z. 2009, ApJ, 701, 1940
- Zhang, F., Qu, J. L., C. M. Zhang, et al. 2006, ApJ, 646, 1116

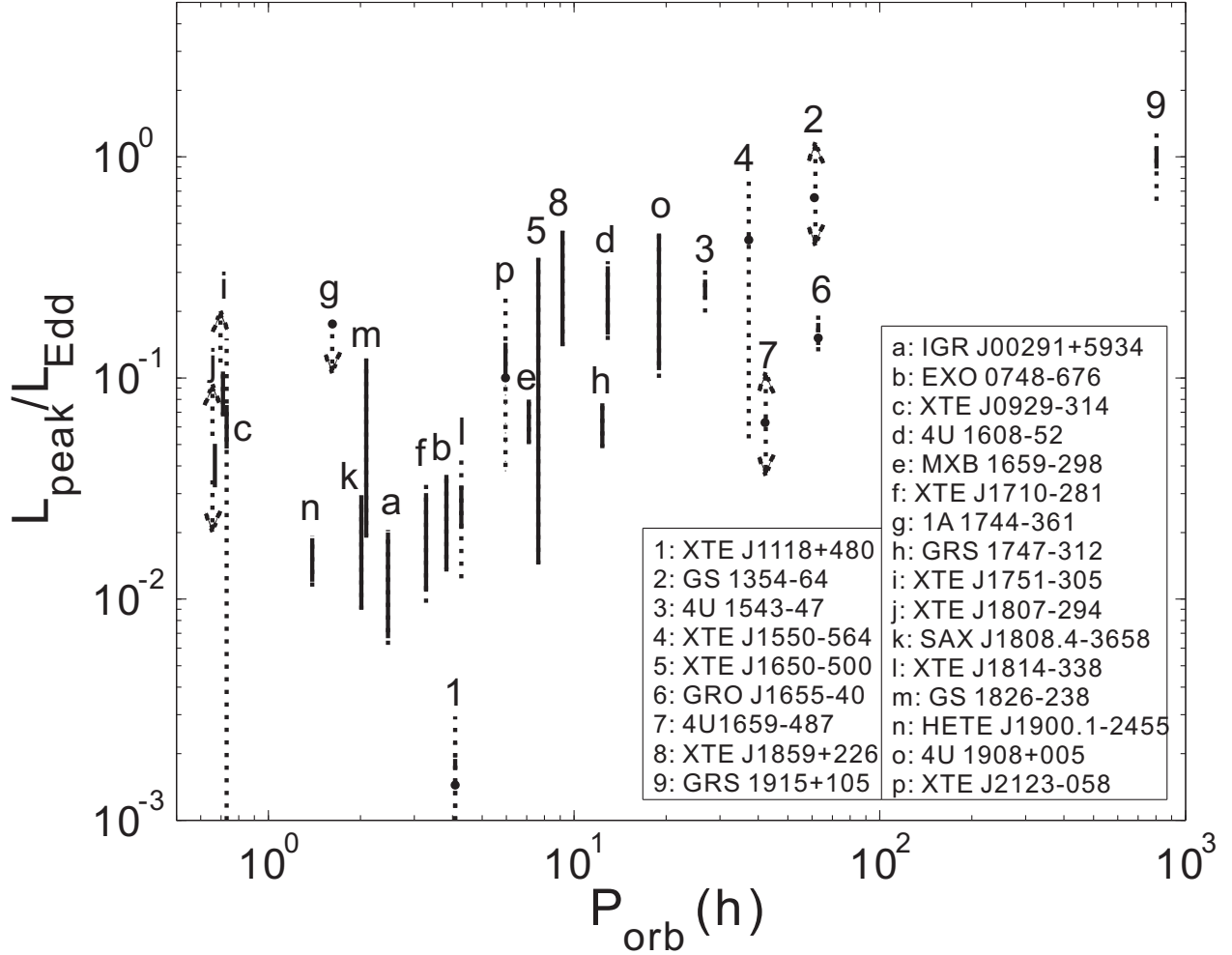


Fig. 1.— The peak luminosity (3–200 keV) as a function of the orbital period. The sources are listed in Table 3. BHs and NSs are marked as numbers and letters respectively, corresponding to the first column of Table 3. Solid line shows the range of the source luminosity and dotted line shows the uncertainty range. Arrow represents the upper or lower limit. Double arrows indicate the values are uncertain.

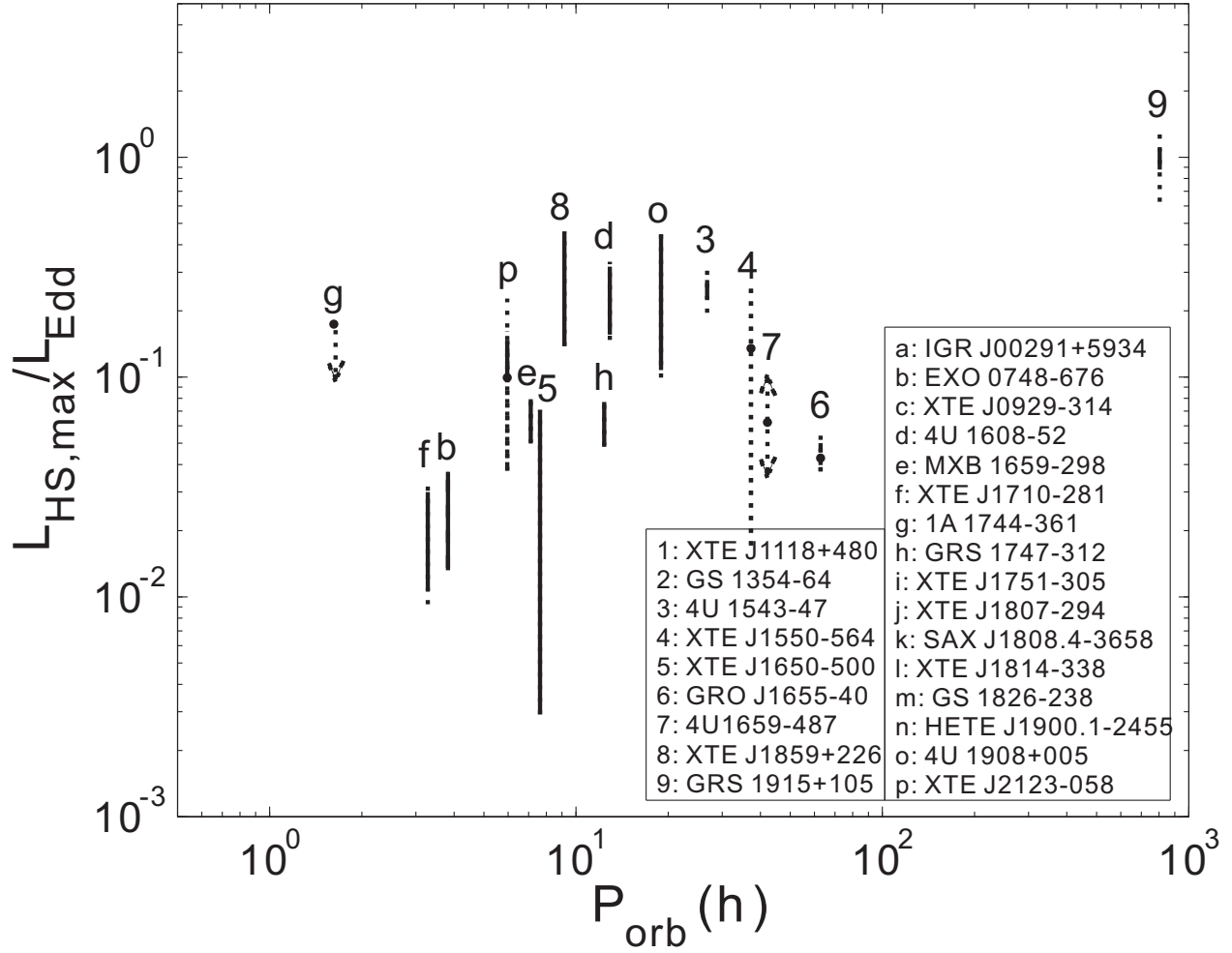


Fig. 2.— The maximal luminosity (3–200 keV) in the HS state as a function of the orbital period. Notation is the same as that in Figure 1.

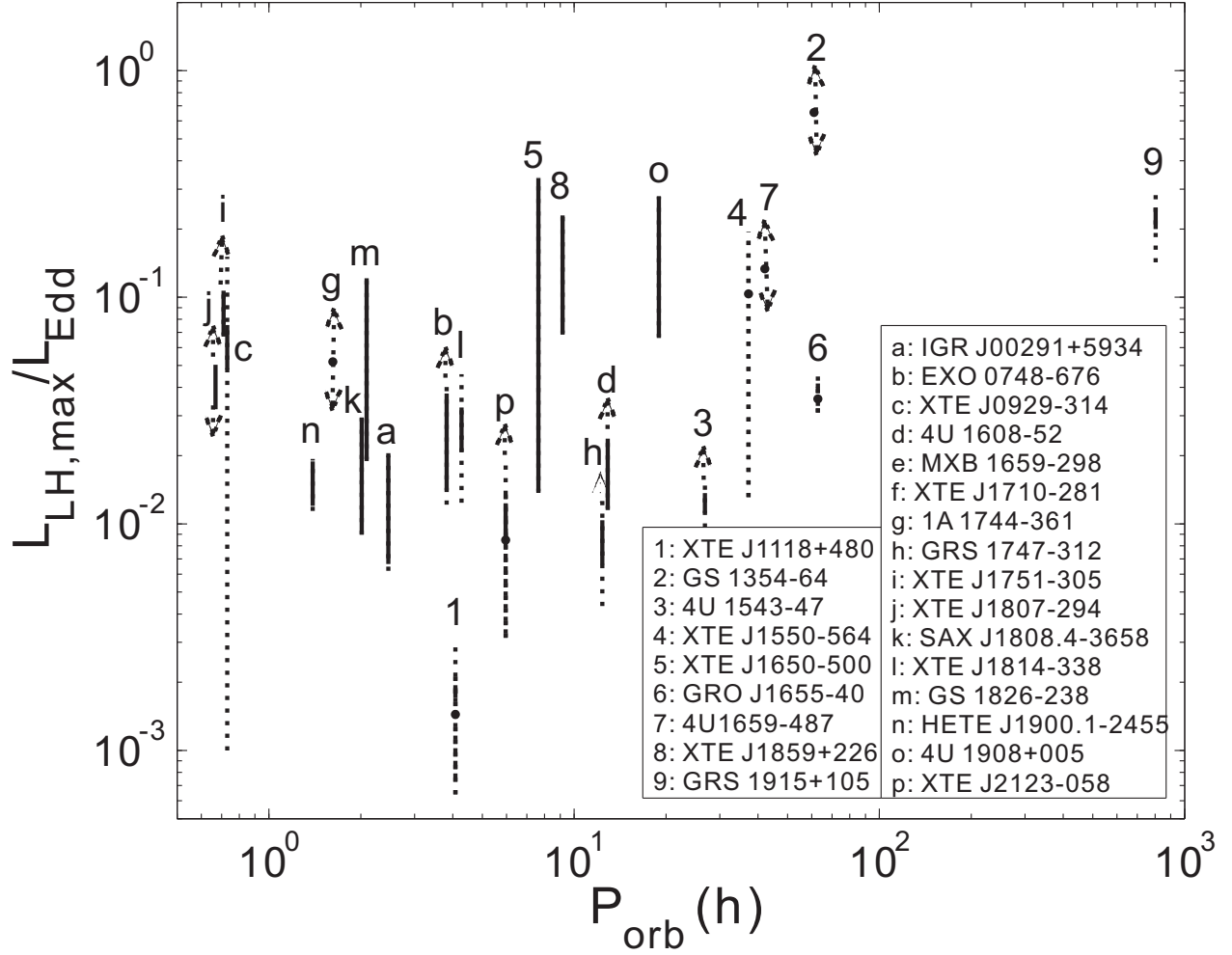


Fig. 3.— The maximal luminosity (3–200 keV) in the LH state as a function of the orbital period. Notation is the same as that in Figure 1. The luminosity of HS-to-LH state transition during the decay of an outburst, is taken and plotted as the lower limit of the maximal LH state luminosity if the LH state in the rise was not observed.

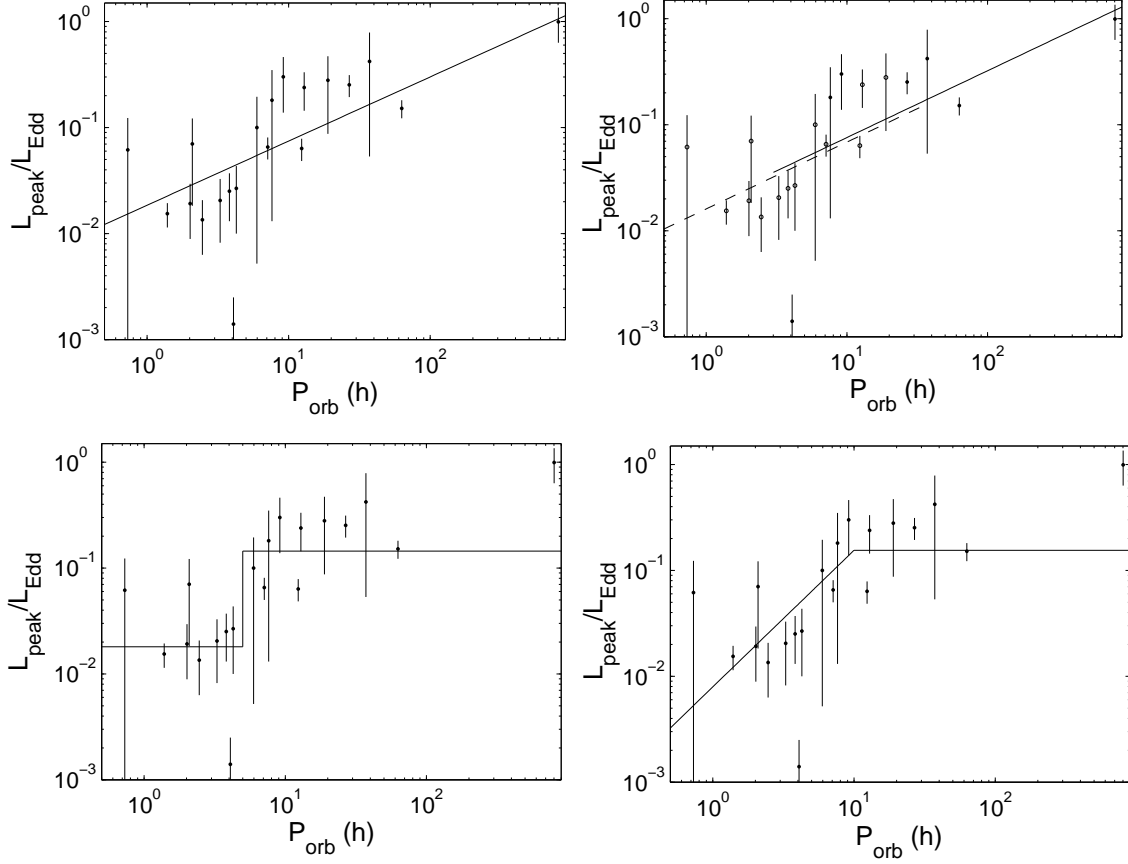


Fig. 4.— *Upper left panel:* the best-fitting linear model for the overall sources in the log scale. *Upper right panel:* the lines fitted to the BHs (shown as a solid line) and NSs (shown as a dashed line). *Lower left panel:* the best-fitting step function. *Lower right panel:* The best-fitting model consisting of a line and a constant, with the break period fixed at 10 h. The uncertain values in Figure 1 (“2”, “7”, “g”, “i”, “j”) have been excluded from fitting for all the cases. In the latter three cases, the outlier at the orbital period of 4.1h, XTE J1118+480 (“1”), is excluded from fitting.

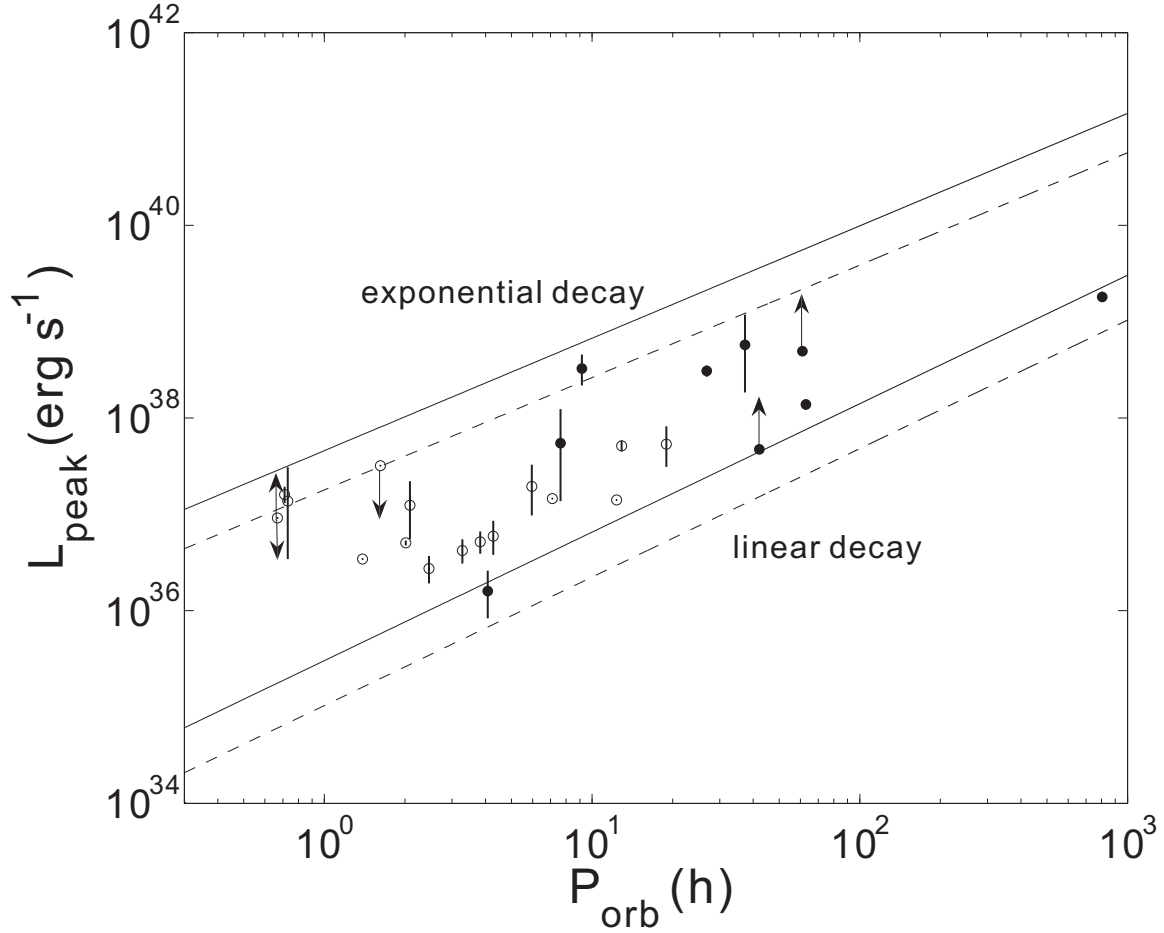


Fig. 5.— The theoretical outburst peak luminosity of SXT as a function of orbital period. The upper pair of lines show the peak luminosity corresponding to the exponential decay, the lower pair corresponding to the linear decay. In each pair, the solid and dashed lines show the peak luminosities for SXTs with primary mass of $10 M_{\odot}$ and $2 M_{\odot}$, typical for BH and NS systems respectively. The sources in Table 3 are also plotted, with dot representing BH and circle representing NS.

Table 1. List of transient LMXBs with known orbital period

Source	Type	Year	$F_x(\mu\text{Jy})(2-10\text{ keV})$	$M(M_\odot)$	$D(\text{kpc})$	$P_{\text{orb}}(\text{hr})$
GRO J0422+32	BH	1992	2800 (8-13 keV)	3.97±0.95	2.49	5.092
A 0620-00	BH	1975	50000	11.0±1.9	1.2	7.75
GRS 1009-45	BH	1993	800 (1-10 keV)	>3.9	1.5-4.5/5.7	6.84
XTE J1118+480	BH	2000,2005	40 (2-12 keV)	8.53	1.8	4.08
GS 1124-684	BH	1991	3000	4-11 ^a	5.9	10.38
GS 1354-64	BH ^b	1987,1997	5-120	5.75(f)	≥27	61.07
4U 1543-47	BH	1971,1983,1992, 2002	<1-15000	8.4-10.4	7.5	26.8
XTE J1550-564	BH	1998,2000,2001, 2002,2003	600-7000	10.5±1.0	5.3	37.25
XTE J1650-500	BH ^c	2001	455 (0.5-10 keV)	<7.3/ 4	2-6/2.6	7.63
GRO J1655-40	BH	1994,1996,2005	1600	7.0/6.3±0.5	3.2/<1.7	62.88
4U 1659-487(GX 339-4)	BH	1972-2007	1.5-900	5.8±0.5(f)	>6	42.14
4U 1705-250	BH	1977	<2-3600	4.86(f)	8.6	12.54
GRO J1719-24	BH ^d	1993,1995	1500 (20-100 keV)	4.9	2.4	14.7
1A 1742-289	BHC	1975	<9-2000	...	10	8.356
CXOGC J174540.0-290031	BHC ^e	2005	0.2(2-8 keV)	7.9
4U 1755-33	BHC	1974-1996	100	...	4-9	4.4
XTE J1859+226	BH	1999	1300	7.4±1.1(f)	7.6	9.16
GRS 1915+105	BH	1992-	300	14±4	11.2-12.5	804
GS 2000+25	BH	1988	<0.5-11000	4.8-14.4	2.7	8.26
GS 2023+338	BH	1989	0.03-20000	12±2	3.5	155.4
IGR J00291+5934	NS (MP)	2004	52 (2.5-25 keV)	...	2.6-3.6	2.46
EXO 0748-676	NS(B)	1985-	0.1-60	...	5.9-7.7	3.82
XTE J0929-314	NS(MP)	2002	36	...	10±5	0.73
4U 1456-32(Cen X-4)	NS(B)	1969,1979	0.1-20000	1.3±0.6/ 1.5±1.0	1.2	15.10
4U 1608-52	NS(B)	1976-	<1-110	...	4.1/3.6	12.89
MXB 1659-298	NS(B)	1976,1999	<5-80	...	10	7.11
XTE J1710-281	NS(B)	1998	2	...	12-16	3.28
1A 1744-361	NS(B)	1976,1989,2003, 2004,2005	<25-275	...	<9	1.62
AX J1745.6-2901	NS(B)	1996	0.4-2 (3-10 keV)	8.4
GRS 1747-312	NS(B)	1990,1996-1999, 2004	1.5-20	...	9.5	12.36
XTE J1751-305	NS(MP)	2002	60 (2-10 keV)	...	~8.5/>7	0.71
XTE J1807-294	NS(MP)	2003	58 (2-10 keV)	0.668
SAX J1808.4-3658	NS(MP,B)	1998,2000,2002, 2005,2008	110	<2.27	2.5/3.4-3.6	2.014167
XTE J1814-338	NS(MP,B)	2003	13	...	8.0±1.6	4.27462
GS 1826-238	NS(B)	1988-	30	...	4-8	2.088
HETE J1900.1-2455	NS(MP,B)	2005	55 (2-20 keV)	...	5	1.39
4U 1908+005 (Aql X-1)	NS(B)	1978-	<0.1-1300	...	5	18.95
XTE J2123-058	NS(B)	1998	110	1.5±0.3/ 1.04-1.56	8.5±2.5	5.96

Note. — ‘Source’—the source name taken from LPH07; ‘Type’—for neutron star, ‘B’ represents X-ray burst source, ‘MP’ represents millisecond pulsar; ‘Year’—the years of outbursts or the year of discovery; ‘ F_x ’—the maximal X-ray flux, or the range of observed X-ray fluxes (2-10 keV, unless otherwise indicated), $1\mu\text{Jy} = 10^{-29} \text{ erg cm}^{-2} \text{ s}^{-1} \text{ Hz}^{-1} = 2.4 \times 10^{-12} \text{ erg cm}^{-2} \text{ s}^{-1} \text{ keV}^{-1}$; ‘ M ’—the mass of the central compact star, the letter ‘f’ in the parentheses indicates the mass function; ‘ D ’—the distance; ‘ P_{orb} ’—the orbit period. The data in the above four columns are from LPH07.

^aFrom Shahbaz et al. (1997) which is taken as reference for BH mass in LPH07

^bClassified as BHC in MR06, but confirmed as BH in Casares et al. (2004).

^cClassified as BHC in MR06, but confirmed as BH in Orosz et al. (2004).

^dClassified as BHC in MR06, but taken as BH in LPH07 with a mass of $4.9 M_{\odot}$ (Masetti et al. 1996).

^eNot listed in MR06, and discovered by Munro et al. (2005).

Table 2. Spectral Parameters of transient LMXBs

Source	State	MJD	ObsID	N_H	T_B	N_B	Γ_{PL}	N_{PL}	$E_{Fe\ line}$	$\sigma_{Fe\ line}$	$N_{Fe\ line}$	χ^2_{ν}/dof	additional details
XTE J1118+480	PLH	51659	50407-01-03-01	0.013	$1.748^{+0.010}_{-0.010}$	$0.298^{+0.006}_{-0.007}$	0.80/99	...
GS 1354-64	PLH	50787	20431-01-04-00	0.7	$1.82^{+0.07}_{-0.07}$	$2.39^{+0.27}_{-0.25}$	$1.12^{+0.06}_{-0.06}$	$0.086^{+0.014}_{-0.013}$	0.95/93	PL cutoff 60 keV
4U 1543-47	P,HS	52445	70133-01-04-00	0.4	$0.979^{+0.005}_{-0.004}$	7876^{+255}_{-132}	$2.63^{+0.02}_{-0.03}$	$5.60^{+0.20}_{-0.39}$	$6.00^{+0.19}_{-0.34}$	$0.83^{+0.04}_{-0.15}$	$.09^{+0.01}_{-0.02}$	1.37/94	...
	LH(d)	52483	70124-02-06-00	0.4	$1.67^{+0.10}_{-0.11}$	$1.14^{+0.31}_{-0.27}$	$1.56^{+0.06}_{-0.06}$	$0.076^{+0.014}_{-0.012}$	1.35/97	...
XTE J1550-564	P,VH	51076	30191-01-02-00	2.0	$4.18^{+0.15}_{-0.16}$	$2.25^{+0.35}_{-0.24}$	$2.92^{+0.01}_{-0.01}$	234^{+6}_{-6}	$5.9^{+0.4}_{-0.5}$	$1.72^{+0.29}_{-0.17}$	$.68^{+23}_{-22}$	1.95/97	smedge at 8.5 keV
	HS	51201	40401-01-19-00	2.0	$1.137^{+0.004}_{-0.004}$	3822^{+85}_{-83}	$2.18^{+0.02}_{-0.02}$	$3.86^{+0.24}_{-0.23}$	1.81/101	...
	LH(r)	51066	30188-06-01-03	2.0	$0.78^{+0.09}_{-0.02}$	1588^{+111}_{-768}	$1.600^{+0.008}_{-0.004}$	$4.56^{+0.14}_{-0.02}$	$6.3^{+0.6}_{-0.3}$	$1.16^{+0.07}_{-0.02}$	$.095^{+0.05}_{-0.02}$	1.84/97	PL cutoff 35 keV
XTE J1650-500	P,VH	52162	60113-01-05-01	0.6	$1.08^{+0.01}_{-0.01}$	176^{+8}_{-11}	$1.52^{+0.02}_{-0.02}$	$1.55^{+0.01}_{-0.01}$	$6.3^{+0.5}_{-0.5}$	$1.42^{+0.03}_{-0.06}$	$.057^{+0.002}_{-0.003}$	1.79/94	PL cutoff 97 keV
	HS	52187	60113-01-25-00	0.6	$0.664^{+0.003}_{-0.003}$	8147^{+201}_{-202}	$2.25^{+0.02}_{-0.02}$	$0.94^{+0.06}_{-0.07}$	6.5(fixed)	$0.69^{+0.11}_{-0.11}$	$.005^{+0.001}_{-0.001}$	1.75/94	smedge at 8 keV
	LH(r)	52158	60113-01-01-00	0.6	$1.66^{+0.09}_{-0.17}$	$21.1^{+6.7}_{-2.6}$	$1.33^{+0.07}_{-0.06}$	$0.85^{+0.15}_{-0.12}$	$6.53^{+0.12}_{-0.17}$	$0.80^{+0.4}_{-0.3}$	$.012^{+0.010}_{-0.004}$	1.52/93	PL cutoff 84
GRO J1655-40	P,VH	53508	91702-01-58-00	0.6	$4.05^{+0.19}_{-0.19}$	$4.4^{+1.1}_{-1.1}$	$2.64^{+0.03}_{-0.03}$	84^{+2}_{-2}	$6.3^{+0.4}_{-0.4}$	$0.87^{+0.15}_{-0.15}$	$.26^{+0.05}_{-0.05}$	2.98/91	smedge at 9 keV, PL cutoff
	HS	53448	91702-01-07-02	0.6	$1.324^{+0.011}_{-0.011}$	1089^{+50}_{-49}	$2.40^{+0.08}_{-0.08}$	$2.55^{+0.74}_{-0.55}$	0.81/94	smedge at 7.1 keV
	LH(r)	53440	91702-01-02-00G	0.6	$1.33^{+0.02}_{-0.02}$	222^{+11}_{-15}	$2.06^{+0.05}_{-0.02}$	$4.7^{+0.3}_{-0.1}$	1.59/96	PL cutoff 144 keV
4U 1659-487	P,HS	52484	70110-01-33-00	0.4	$0.888^{+0.009}_{-0.009}$	3377^{+210}_{-185}	$2.16^{+0.08}_{-0.08}$	$0.43^{+0.09}_{-0.08}$	6.4(fixed)	$0.60^{+0.15}_{-0.19}$	$.009^{+0.003}_{-0.002}$	0.75/94	...
(GX 339-4)	LH(r)	52398	70110-01-09-00	0.4	$1.21^{+0.12}_{-0.06}$	66^{+11}_{-21}	$1.34^{+0.04}_{-0.03}$	$1.05^{+0.07}_{-0.05}$	$6.3^{+1.1}_{-1.1}$	$0.22^{+0.09}_{-0.19}$	$.045^{+0.006}_{-0.011}$	1.29/94	PL cutoff 42 keV
XTE J1859+226	P,HS	51467	40124-01-12-00	0.2	$1.14^{+0.01}_{-0.01}$	841^{+20}_{-81}	$2.54^{+0.02}_{-0.02}$	$15.1^{+0.8}_{-0.7}$	1.41/97	...
	LH(r)	51462	40124-01-04-00	0.2	$1.03^{+0.14}_{-0.11}$	103^{+82}_{-47}	$1.50^{+0.05}_{-0.06}$	$1.18^{+0.13}_{-0.13}$	6.4(fixed)	$1.18^{+0.18}_{-0.18}$	$.023^{+0.001}_{-0.001}$	0.75/94	PL cutoff 45 keV
GRS 1915+105	P,HS	51513	40703-01-40-01	8	$2.79^{+0.11}_{-0.11}$	$14.1^{+3.5}_{-2.7}$	$3.33^{+0.02}_{-0.02}$	328^{+11}_{-11}	6.4(fixed)	$1.27^{+0.1}_{-0.1}$	$.356^{+0.04}_{-0.04}$	1.25/95	...
	LH(r)	51367	40403-01-09-00	8	$0.69^{+0.03}_{-0.01}$	5767^{+1982}_{-1366}	$1.97^{+0.02}_{-0.01}$	$6.50^{+0.23}_{-0.08}$	$6.3^{+1.0}_{-1.0}$	$1.28^{+0.06}_{-0.14}$	$.092^{+0.003}_{-0.014}$	1.49/93	PL cutoff 29 keV
IGR J00291+5934	PLH	53342	90052-03-01-00	0.5	$1.01^{+0.06}_{-0.07}$	$0.0012^{+0.0003}_{-0.0003}$	$1.38^{+0.07}_{-0.08}$	$0.085^{+0.012}_{-0.012}$	1.07/96	PL cutoff 79 keV
EXO 0748-676	HS	53483	91035-01-01-05	0.1	$1.19^{+0.05}_{-0.05}$	$0.0073^{+0.0006}_{-0.0005}$	$3.1^{+0.3}_{-0.2}$	$0.7^{+0.3}_{-0.2}$	6.4(fixed)	$4.59^{+0.3}_{-0.3}$	$.020^{+0.002}_{-0.002}$	0.87/95	...
	LH(d)	53494	91035-01-04-13	0.1	$1.60^{+0.23}_{-0.15}$	$0.0006^{+0.0002}_{-0.0002}$	$1.36^{+0.13}_{-0.15}$	$0.017^{+0.007}_{-0.005}$	0.94/98	...

Table 2—Continued

Source	State	MJD	ObsID	N_{H}	T_{B}	N_{B}	Γ_{PL}	N_{PL}	$E_{\text{Fe line}}$	$\sigma_{\text{Fe line}}$	$N_{\text{Fe line}}$	χ^2_{ν}/dof	additional details
XTE J0929-314	P,LH	52403	70096-03-02-00	0.12	$0.72^{+0.06}_{-0.07}$	$0.0009^{+0.0001}_{-0.0001}$	$1.79^{+0.04}_{-0.04}$	$0.084^{+0.008}_{-0.008}$	1.04/97	...
4U 1608-52	P,HS	50850	30062-03-01-02	1.8	$2.15^{+0.02}_{-0.02}$	$0.25^{+0.01}_{-0.01}$	$3.76^{+0.02}_{-0.02}$	78^{+3}_{-3}	6.4(fixed)	$1.87^{+0.04}_{-0.04}$	$.50^{+0.04}_{-0.04}$	2.37/96	smedge at 9 keV
	LH(d)	50903	30062-01-01-04	1.8	$0.73^{+0.06}_{-0.05}$	$0.0022^{+0.0003}_{-0.0003}$	$1.97^{+0.02}_{-0.02}$	$0.303^{+0.015}_{-0.015}$	6.4(fixed)	$1.10^{+0.15}_{-0.15}$	$.0024^{+0.0005}_{-0.0005}$	0.90/99	...
MXB 1659-298	P,HS	51276	40050-04-05-01	0.2	$2.15^{+0.04}_{-0.04}$	$0.0048^{+0.0001}_{-0.0001}$	$2.76^{+0.03}_{-0.03}$	$0.98^{+0.04}_{-0.04}$	$6.3^{+0.5}_{-0.5}$	$0.97^{+0.13}_{-0.13}$	$.0033^{+0.0009}_{-0.0009}$	2.58/94	...
XTE J1710-281	P,HS	51359	40135-01-43-00	0.24	$1.65^{+0.11}_{-0.11}$	$0.00046^{+0.00005}_{-0.00005}$	$2.52^{+0.08}_{-0.07}$	$0.098^{+0.013}_{-0.012}$	0.54/97	...
1A 1744-361	P,HS	52965	80431-01-03-02	0.3	$2.08^{+0.03}_{-0.03}$	$0.030^{+0.001}_{-0.001}$	$2.9^{+0.08}_{-0.07}$	$2.2^{+0.2}_{-0.2}$	1.44/94	smedge at 6.6 keV
	LH(d)	53103	90058-04-01-00	0.3	$1.60^{+0.12}_{-0.09}$	$0.0011^{+0.0002}_{-0.0002}$	$1.76^{+0.06}_{-0.07}$	$0.064^{+0.011}_{-0.010}$	0.89/98	...
GRS 1747-312	P,HS	51448	40419-01-02-00	0.6	$2.22^{+0.04}_{-0.06}$	$0.0113^{+0.0005}_{-0.0006}$	$2.58^{+0.09}_{-0.08}$	$0.43^{+0.06}_{-0.05}$	0.89/94	smedge at 6.5 keV
	LH(d) ^a	53258	80045-02-10-01	0.6	$1.42^{+0.20}_{-0.29}$	$0.0002^{+0.0001}_{-0.0001}$	$2.08^{+0.17}_{-0.25}$	$0.022^{+0.009}_{-0.010}$	0.94/98	...
XTE J1751-305	P,LH	52369	70131-01-01-00	0.6	$1.38^{+0.08}_{-0.05}$	$0.0020^{+0.0003}_{-0.0004}$	$1.45^{+0.06}_{-0.05}$	$0.164^{+0.015}_{-0.022}$	0.85/96	PL cutoff 38 keV
XTE J1807-294	P,LH	52697	70134-09-02-00	0.3	$1.1^{+0.3}_{-0.1}$	$0.0004^{+0.0002}_{-0.0002}$	$1.72^{+0.08}_{-0.06}$	$0.16^{+0.08}_{-0.02}$	0.90/96	PL cutoff 47 keV
SAX J1808.4-3658	P,LH	52563	70080-01-01-01	0.12	$0.79^{+0.03}_{-0.03}$	$0.0085^{+0.0006}_{-0.0006}$	$1.51^{+0.04}_{-0.05}$	$0.27^{+0.03}_{-0.02}$	6.4(fixed)	$1.14^{+0.13}_{-0.12}$	$.0073^{+0.0012}_{-0.0012}$	0.98/94	PL cutoff 37 keV
XTE J1814-338	P,LH	52818	80418-01-04-01	0.15	$1.15^{+0.09}_{-0.09}$	$0.0004^{+0.0002}_{-0.0002}$	$1.49^{+0.14}_{-0.09}$	$0.052^{+0.008}_{-0.012}$	0.86/96	PL cutoff 54 keV
GS 1826-238	P,LH	52484	70044-01-01-01	0.17	$1.34^{+0.17}_{-0.09}$	$0.0014^{+0.0004}_{-0.0005}$	$1.29^{+0.08}_{-0.06}$	$0.14^{+0.02}_{-0.01}$	1.07/96	PL cutoff 35 keV
HETE J1900.1-2455	P,LH	53553	91015-01-05-00	0.10	$1.11^{+0.03}_{-0.03}$	$0.0026^{+0.0004}_{-0.0003}$	$1.41^{+0.12}_{-0.15}$	$0.075^{+0.018}_{-0.018}$	1.31/97	PL cutoff 33 keV
4U 1908+005	P,HS	51834	50049-02-04-00	0.3	$1.97^{+0.02}_{-0.02}$	$0.154^{+0.004}_{-0.004}$	$3.89^{+0.07}_{-0.07}$	49^{+4}_{-5}	6.4(fixed)	$1.62^{+0.11}_{-0.093}$	$.22^{+0.03}_{-0.03}$	1.90/92	smedge at 6 keV
(Aql X-1)	LH(r)	51820	50049-01-04-03	0.3	$1.39^{+0.07}_{-0.08}$	$0.010^{+0.004}_{-0.004}$	$1.29^{+0.08}_{-0.08}$	$0.68^{+0.12}_{-0.11}$	6.4(fixed)	$1.16^{+0.23}_{-0.27}$	$.016^{+0.006}_{-0.006}$	0.83/94	PL cutoff 23 keV
XTE J2123-058	P,HS	50991	30511-01-01-00	0.06	$1.91^{+0.04}_{-0.04}$	$0.0109^{+0.0004}_{-0.0004}$	$2.51^{+0.05}_{-0.05}$	$0.99^{+0.09}_{-0.08}$	1.37/101	...
	LH(d)	51040	30511-01-06-00	0.06	$0.88^{+0.06}_{-0.07}$	$0.00015^{+0.00004}_{-0.00003}$	$1.72^{+0.01}_{-0.02}$	$0.015^{+0.001}_{-0.001}$	0.82/101	...

Note. — ‘Source’—the source name. The sources above and under the horizontal line are BH systems and NS systems respectively. ‘State’—the location and state of the observation. The letter ‘P’ indicates the observation corresponds to the outburst peak, of which the spectral state is one of the followings: the very high state (VH), the high/soft state (HS) and the low/haed state (LH). The observation without the letter ‘P’ has the maximal flux of the corresponding state. The letter ‘r’ or ‘d’ in the parentheses indicates the LH state is during the rising or decaying phase of an outburst. ‘MJD’—the MJD of the observation. ‘ObsID’—the observation ID of the *RXTE* pointed observation. ‘ N_{H} ’—the hydrogen column density, in units of 10^{-22} cm^{-2} . ‘ T_{B} ’—the temperature at inner disk radius in “diskbb” model for BH systems, or the temperature of blackbody in “bbody” model for NS systems, in the units of keV. ‘ N_{B} ’—the normalization of “diskbb” model for BH systems or “bbody” model for NS systems, see the Xspec manual for details. ‘ Γ_{PL} ’—the photon index of powerlaw. ‘ N_{PL} ’—the normalization of powerlaw, photons $\text{keV}^{-1} \text{ cm}^{-2} \text{ s}^{-1}$ at 1 keV. ‘ $E_{\text{Fe line}}$ ’—the energy of Fe line, in the units of keV. ‘ $\sigma_{\text{Fe line}}$ ’—the width of Fe line, in the units of keV. ‘ $N_{\text{Fe line}}$ ’—normalization of Fe line, in the units of photons $\text{cm}^{-2} \text{ s}^{-1}$. ‘ χ^2_{ν}/dof ’—reduced chi-square/degrees of freedom. ‘additional details’—additional component of the spectrum. The error of each fitted parameter corresponds to the 90% confidence region.

^aThe decay of a different outburst.

Table 3. Parameters and Fluxes of transient LMXBs Plotted in Figure 2–4

Mark	Sources	P_{orb} (hr)	$M(M_{\odot})^b$	$D(\text{kpc})$	F_{peak}	$F_{\text{HS,max}}$	$F_{\text{LH,max}}$
1	XTE J1118+480	4.08	$8.53 \pm 0.06 / 6.5\text{-}7.2[\text{M}]$	$1.8 \pm 0.5[\text{M}]$	$4.12^{+0.11}_{-0.09}$...	$4.12^{+0.11}_{-0.09}$
2	GS 1354-64	61.07	≥ 5.75	≥ 27	$5.60^{+0.05}_{-0.12}$...	$5.60^{+0.05}_{-0.12}$
3	4U 1543-47	26.8	8.5-10.4	$7.5 \pm 0.5[\text{M}]$	$45.76^{+0.17}_{-0.17}$	$45.76^{+0.17}_{-0.17}$	$2.24^{+0.05}_{-0.08}$
4	XTE 1550-564	37.25	10.5 ± 1.0	$5.3 \pm 2.3[\text{M}]$	$170.9^{+2.1}_{-2.2}$	$58.18^{+0.16}_{-0.17}$	$42.0^{+0.6}_{-0.6}$
5	XTE J1650-500	7.63	2.73-7.3 ^a	2-6	$28.62^{+0.20}_{-0.20}$	$5.86^{+0.04}_{-0.04}$	$27.6^{+0.3}_{-0.4}$
6	GRO J1655-40	62.88	$7.02 \pm 0.22 / 6.0\text{-}6.6[\text{M}]$	$3.2 \pm 0.2[\text{M}]$	$112.9^{+1.5}_{-1.3}$	$32.1^{+0.3}_{-0.3}$	$26.50^{+0.08}_{-0.10}$
7	4U 1659-487	42.14	≥ 5.8	> 6	$10.99^{+0.09}_{-0.07}$	$10.99^{+0.09}_{-0.07}$	$23.4^{+0.5}_{-0.5}$
8	XTE J1859+226	9.16	7.6-12.0[M]	7.6/11[M]	$31.51^{+0.11}_{-0.12}$	$31.51^{+0.11}_{-0.12}$	$15.66^{+0.20}_{-0.24}$
9	GRS 1915+105	804	14 ± 4	11.2-12.5	$107.4^{+0.4}_{-0.4}$	$107.4^{+0.4}_{-0.4}$	$24.2^{+0.4}_{-0.4}$
a	IGR J00291+5934	2.46	...	2.6-3.6	$2.35^{+0.06}_{-0.16}$...	$2.35^{+0.06}_{-0.16}$
b	EXO 0748-676	3.82	...	5.9-7.7	$0.936^{+0.023}_{-0.022}$	$0.936^{+0.023}_{-0.022}$	$0.97^{+0.009}_{-0.13}$
c	XTE J0929-314	0.73	...	10 ± 5	$1.15^{+0.05}_{-0.05}$...	$1.15^{+0.05}_{-0.05}$
d	4U 1608-52	12.89	...	4.1/3.6	$29.0^{+1.6}_{-1.6}$	$29.0^{+1.6}_{-1.6}$	$2.150^{+0.031}_{-0.033}$
e	MXB 1659-298	7.11	...	10	$1.215^{+0.018}_{-0.014}$	$1.215^{+0.018}_{-0.014}$...
f	XTE J1710-281	3.28	...	12-16	$0.179^{+0.024}_{-0.019}$	$0.179^{+0.024}_{-0.019}$...
g	1A 1744-361	1.62	...	< 9	$3.29^{+0.22}_{-0.22}$	$3.29^{+0.22}_{-0.22}$	$0.98^{+0.07}_{-0.07}$
h	GRS 1747-312	12.36	...	9.5	$1.294^{+0.022}_{-0.020}$	$1.294^{+0.022}_{-0.020}$	$0.17^{+0.05}_{-0.06}$
i	XTE J1751-305	0.71	...	8.5/ > 7	$2.25^{+0.02}_{-0.03}$...	$2.25^{+0.02}_{-0.03}$
j	XTE J1807-294	0.668	...	8 ^c	$1.20^{+0.02}_{-0.04}$...	$1.20^{+0.02}_{-0.04}$
k	SAX J1808.4-3658	2.014/167	< 2.27	2.5/3.4-3.6	$3.44^{+0.19}_{-0.22}$...	$3.44^{+0.19}_{-0.22}$
l	XTE J1814-338	4.274/62	...	8.0 ± 1.6	$0.78^{+0.02}_{-0.04}$...	$0.78^{+0.02}_{-0.04}$
m	GS 1826-238	2.088	...	4-8	$2.88^{+0.04}_{-0.05}$...	$2.88^{+0.04}_{-0.05}$
n	HETE J1900.1-2455	1.39	...	5	$1.15^{+0.03}_{-0.06}$...	$1.15^{+0.03}_{-0.06}$
o	4U 1908+005	18.95	...	5(4-6.5)	$16.2^{+1.2}_{-1.2}$	$16.2^{+1.2}_{-1.2}$	$9.98^{+0.08}_{-0.11}$
p	XTE J2123-058	5.96	$1.5 \pm 0.3 / 1.04\text{-}1.56$	8.5 ± 2.5	$2.26^{+0.07}_{-0.06}$	$2.26^{+0.07}_{-0.06}$	$0.191^{+0.018}_{-0.020}$

Note. — The first column is the mark of a source (number for BH and letter for NS), which is used in Figure 1–3. The mass and distance data are from LPH07 and references therein, except those marked with ‘M’ in the square brackets which are from MR06. ‘ F_{peak} ’, ‘ $F_{\text{HS,max}}$ ’, ‘ $F_{\text{LH,max}}$ ’ are the unabsorbed fluxes of outburst peak, the HS state maximum and the LH state maximum respectively, in the units of 10^{-9} erg cm^{-2} s^{-1} .

^aMass function $f(M)=2.73 M_{\odot}$ and the BH mass $< 7.3 M_{\odot}$ (LPH07).

^bThe mass of NS is assumed in the range of 1.4–2.2 M_{\odot} if it is not known.

^cThe distance is unknown, but usually assumed as 8 kpc as the source might be close to the Galactic center (e.g. Campana et al. 2003; Falanga et al. 2005).